Correspondence

Completed Local Binary Count for Rotation Invariant Texture Classification

Yang Zhao, De-Shuang Huang, *Senior Member, IEEE*, and Wei Jia, *Member, IEEE*

***Abstract*— In this brief, a novel local descriptor, named local binary count (LBC), is proposed for rotation invariant texture classification. The proposed LBC can extract the local binary grayscale difference information, and totally abandon the local binary structural information. Although the LBC codes do not represent visual microstructure, the statistics of LBC features can represent the local texture effectively. In addition, a completed LBC (CLBC) is also proposed to enhance the performance of texture classification. Experimental results obtained from three databases demonstrate that the proposed CLBC can achieve comparable accurate classification rates with completed local binary pattern.**

***Index Terms*— Local binary pattern (LBP), local binary count (LBC), rotation invariance, texture classification.**

I. Introduction

Texture classification is very useful in many applications, such as remote sensing, biomedical image analysis, image recognition and retrieval. Thus, it is an important issue in image processing and computer vision. Generally, texture images captured in the real world may have obvious orientation variations. Rotation invariant texture analysis is therefore immensely needed from both the practical and theoretical viewpoints.

So far, many approaches have been proposed to achieve rotation invariance for texture classification which can be broadly divided into two categories, i.e., statistical methods and model based methods, respectively. In statistical methods, texture is generally described by the statistics of selected features, e.g., invariant histogram, texture elements, and micro-structures. Davis et al [1] exploited polarograms and generalized co-occurrence matrices to obtain rotation invariant statistical features. Duvernoy et al [2] proposed Fourier descriptors to extract the rotation invariant texture feature on the spectrum domain. Goyal et al [3] proposed a method by using texel property histogram. Eichmann et al [4] presented texture descriptors based on line structures extracted by Hough transform. In model based methods, texture is usually presented as a probability model or as a linear combination of a set of basis functions. Kashyap et al [5] developed a circular simultaneous autoregressive (CSAR) model for rotation invariant texture classification. Cohen et al [6] characterized texture as Gaussian Markov random fields and used the maximum likelihood to estimate rotation angles. Chen and Kundu [7] addressed rotation invariant by using multichannel sub-bands decomposition and hidden Markov model (HMM). Porter et al [8] exploited the wavelet transform for rotation invariant texture classification by using the Daubechies four-tap wavelet filter coefficients.

Although these aforementioned methods are proven to be rotation invariant, they are not very robust to variances of illumination. In [9], Ojala et al proposed an efficient method, namely Local Binary Pattern (LBP), for rotation invariant texture classification. As shown in Fig. 1, the algorithm of LBP contains two main steps, i.e., thresholding step and encoding step. In the thresholding step, the values of neighbor pixels are turned to binary values (0 or 1) by comparing them with the central pixel. Obviously, the local binary grayscale difference information is extracted in the thresholding step. In the encoding step, the binary numbers are encoded to characterize a structural pattern, and then the code is transformed into decimal number. Aiming at achieving rotation invariance, Ojala proposed rotation invariant uniform LBP (LBP^{riu2}), in which only rotation invariant uniform local binary patterns were selected. It was believed that LBP is an excellent measure of the spatial structure of local image texture since it can effectively detect micro-structures (e.g., edges, lines, spots) information.

Since Ojala's work [9], a lot of variants of the LBP for rotation invariant texture classification have been proposed, some of which were focused on how to extract more discriminative patterns. For example, Heikkila et al [10] proposed center-symmetric LBP (CS-LBP) by comparing center-symmetric pairs of pixels instead of comparing neighbors with central pixels. Liao et al [11] presented Dominant LBP (DLBP), in which dominant patterns were experimentally chosen from all rotation invariant patterns. Others tried to further explore the contrast information. For example, Tan and Triggs [12] proposed the method of Local Ternary Pattern (LTP), which extends original LBP to 3-valued codes. Recently, Guo et al [13] proposed the completed LBP (CLBP) by combining the conventional LBP with the measures of local intensity difference and central gray level. Khellah [14] presented a new method for texture classification, which combines Dominant Neighborhood Structure (DNS) and traditional LBP. It should be noticed that the LBP encoding process is used in all of these variants mentioned above because it is believed that structural patterns characterized by the binary codes are more important for rotation invariant texture recognition while local binary grayscale difference information is considered to be merely a supplement of micro-structures. Recently, there is also another way to look at LBP, e.g., LBP is regarded as a special filter-based texture operator [19], [20].

Then, is micro-structure information really the main role in LBP for rotation invariant texture recognition? It seems that nobody has investigated this problem in depth so far. In this paper, we shall try to address this question by proposing a new local operator that discards the structural information from LBP operator, which is named as Local Binary Count (LBC). Experimental results illustrate that the most discriminative information of local texture for rotation invariant texture classification is not the 'micro-structures' information but the local binary grayscale difference information. Motivated by the

Manuscript received October 17, 2011; revised May 2, 2012; accepted May 20, 2012. Date of publication June 12, 2012; date of current version September 13, 2012. This work was supported by the National Science Foundation of China, under Grant 61133010, Grant 31071168, Grant 61005010, Grant 60905023, and Grant 60975005, and the China Post-Doctoral Science Foundation under Grant 20100480708. The associate editor coordinating the review of this manuscript and approving it for publication was Prof. Zhou Wang.

Y. Zhao is with the Department of Automation, University of Science and Technology of China, Hefei 230027, China, and also with the Hefei Institute of Intelligent Machines, Chinese Academy of Science, Hefei 230031, China (e-mail: zyknight@mail.ustc.edu.cn).

D.-S. Huang is with the School of Electronics and Information Engineering, Tongji University, Shanghai 201804, China (e-mail: dshuang@tongji.edu.cn).

W. Jia is with the Hefei Institute of Intelligent Machines, Chinese Academy of Science, Hefei 230031, China (e-mail: icg.jiawei@gmail.com).

Digital Object Identifier 10.1109/TIP.2012.2204271

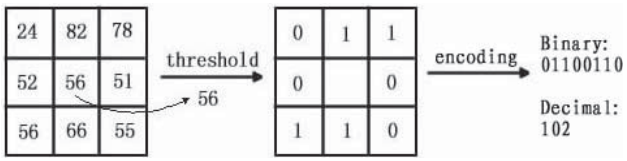

Fig. 1. Illustration of LBP process.

CLBP [13], we also proposed a completed LBC (CLBC). Compared with the CLBP, the proposed CLBC can achieve comparable accurate classification rates. In addition, the proposed CLBC allows slight computational savings in the process of training and classification.

The rest of this paper is organized as follows: Section II briefly reviews the basic principle of the LBP and the CLBP. Section III presents the LBC and the CLBC in detail. Experimental results are presented in Section IV. And Section V concludes the paper with some conclusive remarks.

II. Brief Review of the LBP and the CLBP

In this Section, we provide a brief review of the LBP and the CLBP. As we have mentioned above, the CLBP is a method which extends original LBP to a completed framework and can achieve impressive classification results.

A. Local Binary Pattern (LBP)

Usually, the LBP coding strategy can be described as follows:

$$LBP_{P,R} = \sum_{p=0}^{P-1} s(g_p - g_c)2^p, \quad s(x) = \begin{cases} 1, x \geq 0 \\ 0, x < 0 \end{cases} \tag{1}$$

where g_c represents the gray value of the center pixel and $g_p (p = 0,\ldots, P\text{-}1)$ denotes the gray value of the neighbor pixel on a circle of radius R, and P is the total number of the neighbors. It should be noted that the neighbors that do not fall in the center of pixels can be estimated by bilinear interpolation.

In [9], the rotation invariant LBP is usually defined as:

$$LBP^{\text{ri}}_{P,R} = \min\{ROR(LBP_{P,R}, i)|, \quad i = 0, 1, \ldots, P-1\} \tag{2}$$

where $ROR(x, i)$ performs a circular bit-wise right shift on the P-bit number x i times.

Further, Ojala et al observed that certain patterns provide the vast majority, sometimes over 90 percent among all LBP patterns [9]. Thus they defined a uniformity measure U, which corresponds to the number of spatial transitions (bitwise 0/1 changes) in the pattern as follows:

$$U(LBP_{P,R}) = \left|s(g_{P-1} - g_c) - s(g_0 - g_c)\right| + \sum_{p=1}^{P-1} \left|s(g_P - g_c) - s(g_{p-1} - g_c)\right|. \tag{3}$$

The uniform patterns refer to those patterns which have U values of at most 2 while the remaining non-uniform patterns are all classified into an additional class.

The rotation invariant forms of the uniform patterns are called LBP^{riu2}, where superscript $^{\text{riu2}}$ refers to the rotation invariant uniform patterns. Since rotation invariant is very necessary for texture classification, we shall mainly discuss rotation invariant LBP patterns in this paper.

After the LBP^{riu2} code of each pixel is defined, a histogram will be built to represent the texture image.

B. Completed LBP (CLBP)

In order to improve the discrimination capability of LBP descriptor, Guo et al [13] proposed CLBP descriptor by decomposing the image local differences into two complementary components, i.e., the signs (s_p) and the magnitudes (m_p), respectively:

$$s_p = s(g_p - g_c), \quad m_p = \left|g_p - g_c\right| \tag{4}$$

where g_p, g_c and $s(x)$ are defined as in Eqn. (1). Two operators named CLBP-Sign (CLBP_S) and CLBP-Magnitude (CLBP_M), respectively, are proposed to code them, where the CLBP_S is equivalent to the conventional LBP, and the CLBP_M measures the local variance of magnitude. The CLBP_M can be defined as follows:

$$CLBP\_M_{P,R} = \sum_{p=0}^{P-1} t(m_p, c)2^p, \quad t(x, c) = \begin{cases} 1, & x \geq c \\ 0, & x < c \end{cases} \tag{5}$$

where the threshold c is set as the mean value of m_p of the whole image. Guo et al observed that the center pixel, which expresses the image local gray level, also has discriminative information. Thus, they defined an operator named CLBP-Center (CLBP_C) to extract the local central information as follows:

$$CLBP\_C_{P,R} = t(g_c, c_I) \tag{6}$$

where threshold c_I is set as the average gray level of the whole image. By combining the three operators of the CLBP_S, the CLBP_M and the CLBP_C, significant improvement is made for rotation invariant texture classification.

III. Local Binary Count

A. Local Binary Count (LBC)

In the original LBP and its variants, each pixel in the local neighbor set is turned to binary form by comparing it with the central pixel. Then these binary values are encoded to form the local binary patterns. In the proposed LBC, we only count the number of value 1's in the binary neighbor sets instead of encoding them. The working principle of LBC is illustrated in Fig. 2. The number of value 1's is 4 in the binary neighbor set, thus the LBC code of the central pixel is also 4.

As a result, we can define the computing process for the LBC as follows:

$$LBC_{P,R} = \sum_{p=0}^{P-1} s(g_p - g_c), \quad s(x) = \begin{cases} 1, & x \geq 0 \\ 0, & x < 0 \end{cases} \tag{7}$$

where g_c, g_p, P, and R are the variables, as defined in Eqn. (1). In fact, the main difference between the LBP and the LBC is that the LBP is to use the binary number to encode local patterns while the LBC merely counts the number of value 1's in local neighbor set. But their meanings are very different. Usually, the LBP is to focus on the local structural information characterized by various patterns, while the LBC is only involved in the fact that how many pixels have comparatively higher gray level than the central one in local area. In other words, the LBP can extract the local structure information, while the LBC is merely to focus on the local binary grayscale difference information. Actually, local binary grayscale difference information is a comparative relation after intensity quantization in local neighbor set.

In statistical texture analysis methods, macroscopic textures can be regarded as the repeats for a large number of local microcosmic

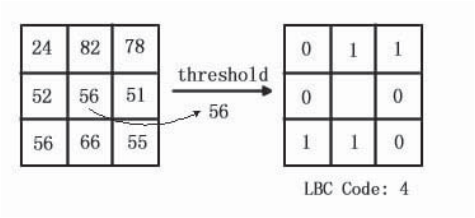

Fig. 2. Illustration of LBC (P = 8, R = 1).

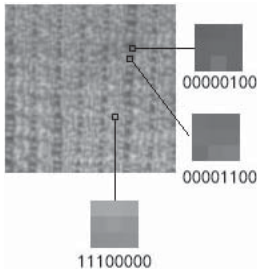

Fig. 3. Schematic diagram of macroscopic textural structure that is quite different from the micro-structure.

patterns. Thus, the statistics of the selected local microcosmic patterns can characterize the whole texture. But the "micro-structure" is quite different from macroscopic textural structure. As illustrated in Fig. 3, the micro-structures, "00000100" and "00001100," may be contained in a macroscopic "line" in texture image, and a micro-structure "line" (e.g., "11100000") may be a "spot" in the image. That is, a macroscopic textural structure in the real image may consist of many different local binary micro-structures. Different macroscopic textural structures may consist of many similar micro-structures, but the frequencies of occurrences of these micro-structures are different. Thus, macroscopic textural structure can be characterized by the statistics of the micro-structures, but not the micro-structures themselves. It is often believed that the local binary pattern can characterize the local texture effectively by detecting "micro-structure" [9]. But these micro-structures do not represent the macroscopic textural structures directly. The LBP characterizes the distribution of local pixels effectively by using the local binary encoding. Thus, the frequency of occurrences of different LBPs can be used to characterize various textural structures. That is the potential reason why LBP performs well in texture analysis. Although the LBC codes don't represent visual micro-structure, the LBC features can distinguish the different distributions of local pixels. Thus, the statistics of the LBC features can also be used to represent the macroscopic textural structures.

There are some reasons why the LBC totally abandons the micro-structure information. Firstly, the micro-structure has the complementary discrimination capability, but not all of the structural patterns are used for rotation invariant texture classification. In experiments it can be found that the number of the specified rotation invariant structural patterns is too few to contain abundant structural information. Secondly, although the rotation invariant patterns, i.e., LBP^{ri} and LBP^{riu2}, are selected, they are not absolutely invariant to rotation. As shown in Fig. 4, some rotation invariant patterns may change after rotation and interpolation, but their LBC codes are stable.

B. Completed Local Binary Count (CLBC)

Similar to the CLBP, we also proposed Completed Local Binary Count (CLBC) to extract completed local textural information, which

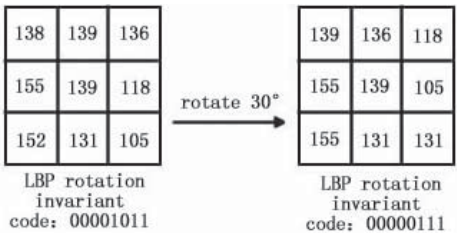

Fig. 4. Rotation invariant codes in LBP may be not stable after rotation.

contains three operators: CLBC-Sign (CLBC_S), CLBC-Magnitude (CLBC_M) and CLBC-Center (CLBC_C). Generally, the CLBC_S equals to the original LBC described above. In order to code the CLBC_M in a consistent format with that of the CLBC_S, the CLBC_M can be defined as:

$$CLBC\_M_{P,R} = \sum_{p=0}^{P-1} s(m_p - c), \quad m_p = \left|g_p - g_c\right| \tag{8}$$

where g_p, g_c, and $s(x)$ are defined as in Eqn.(1), and c denotes the mean value of m_p in the whole image. The CLBC_M counts how many neighbors have comparatively much higher intensity than the center pixel. Thus it is used to extract additional information of the local intensity differences.

In [13], it has been proven that the center pixel can be used to express the local gray level in the image. Thus the CLBC_C can be defined identical to the CLBP_C.

In [13], two ways were used to combine different operators, i.e., jointly and hybridly, respectively. Here, we use the same way to combine the operators of the CLBC_S, the CLBC_M and the CLBC_C. In the first way, we denote 'CLBC_S_M' as the two dimensional joint (2D-joint) of the CLBP_S and the CLBP_M. In the second way, three dimensional joint (3D-joint) is built for the three operators, denoted by 'CLBC_S/M/C'.

IV. Experiments and Discussions

To prove the local binary grayscale difference information plays a main role in texture classification, we carried out a series of experiments on three large and representative databases: the Outex database [15], Columbia-Utrecht Reflection and Texture (CUReT) database [16] and UIUC database [18].

A. Dissimilarity Measure and Multiscale Framework

In this paper, we utilized the χ^2 statistics as the dissimilarity between two histograms. The χ^2 statistics is a bin-by-bin distance, which means only the pairs of bins that have the same index are matched. If $H = \{h_i\}$ and $K = \{k_i\}$ $(i = 1, 2 \ldots B)$ denote two histograms, then χ^2 statistics can be calculated as follows:

$$d_{\chi^2}(H, K) = \sum_{i=1}^{B} \frac{(h_i - k_i)^2}{h_i + k_i}. \tag{9}$$

In [9], [13], a simple multi-resolution framework is used to improve the classification accuracy, that is, by measuring the dissimilarity as the sum of chi-square distances from all operators of various (P, R).

In this paper, assuming that all the methods used the nearest neighborhood classifier for classification. The source codes for the proposed method can be downloaded from our constructed website: http://home.ustc.edu.cn/~zyknight/CLBC.rar.

TABLE I
CLASSIFICATION RATES (%) ON TC10 AND TC12 DATASETS

	R = 1, P = 8				R = 2, P = 16				R = 3, P = 24			
	TC10	TC12		Average	TC10	TC12		Average	TC10	TC12		Average
		t184	horizon			t184	horizon			t184	horizon	
LTP	94.14	75.88	73.96	81.33	96.95	90.16	86.94	91.35	98.2	93.59	89.42	93.74
LBP^{ri}	78.8	71.97	69.98	73.58	91.72	88.26	88.47	89.48	–	–	–	–
LBP/VAR	96.56	79.31	78.08	84.65	97.84	85.76	84.54	89.38	98.15	87.13	87.08	86.96
CLBP_S	84.81	65.46	63.68	71.31	89.40	82.26	75.20	82.28	95.07	85.04	80.78	86.96
CLBC_S	82.94	65.02	63.17	70.38	88.67	82.57	77.41	82.88	91.35	83.82	82.75	85.97
CLBP_M	81.74	59.3	62.77	67.93	93.67	73.79	72.40	79.95	95.52	81.18	78.65	85.11
CLBC_M	78.96	53.63	58.01	63.53	92.45	70.35	72.64	78.48	91.85	72.59	74.58	79.67
CLBP_S_M	94.66	82.75	83.14	86.85	97.89	90.55	91.11	93.18	99.32	93.58	93.35	95.41
CLBC_S_M	95.23	82.13	83.59	86.98	98.10	89.95	90.42	92.82	98.7	91.41	90.25	93.45
CLBP_S/M/C	96.56	**90.30**	92.29	93.05	98.72	93.54	93.91	95.39	98.93	95.32	94.53	96.26
CLBC_S/M/C	**97.16**	89.79	**92.92**	93.29	98.54	93.26	94.07	95.29	98.78	94.00	93.24	95.67
CLBC_CLBP	96.88	90.25	**92.92**	**93.35**	**98.83**	**93.59**	**94.26**	**95.56**	**98.96**	**95.37**	**94.72**	**96.35**
DLBP[11]	–	–	–	–	97.7	92.1	88.7	92.83	98.1	91.6	87.4	92.37

B. Experimental Results on Outex Database

When conducting the experiments on Outex database, we used the Outex test suits Outex_TC_0010 (TC10) and Outex_TC_0012 (TC12), where TC10 and TC12 contain 24 classes of texture images captured under three illuminations ("inca","tl84" and "horizon") and nine rotation angles (0°, 5°, 10°, 15°, 30°, 45°, 60°, 75°, and 90°). There are twenty 128×128 images for each rotation angle under a given illumination condition. The 24 × 20 images of illumination "inca" and rotation angle 0° were adopted as the training data. For TC10 dataset the other 8 rotation angles with illumination "inca" were used for test. For TC12 dataset, all the samples captured under illumination "tl84" or "horizon" were used as the test data.

Table I lists the experimental results of different methods, from which we could get some interesting findings. Firstly, the CLBC_S and the CLBP_S, the CLBC_M and the CLBP_M achieve similar accurate classification rates, respectively. Secondly, better classification rates than the ones obtained by LTP, LBP/VAR and DLBP can be achieved by combining 'Magnitude' with 'Sign' jointly or hybridly. In 2D-joint way, the CLBC_S_M and the CLBP_S_M can get similar classification rates. In the 3D-joint way, the CLBP_S/M/C and the CLBC_S/M/C achieve much better results than the other listed methods. The CLBP_S/M/C is slightly better than the CLBC_S/M/C under illumination 'inca' and 'tl84'. But their average performances still stay at the same level. Lastly, it can be found that the combination of the CLBC_S/M/C and the CLBP_S/M/C (the CLBC_CLBP) can perform slightly better than the one each individual does.

By applying the multi-scale scheme, some better results could be obtained. It can be found that the multi-scale CLBP can reach the classification rates of 99.14%, 95.18% and 95.55% for TC10, 'tl84' and 'horizon', respectively. The multi-scale CLBC can reach the ones of 99.38%, 94.98% and 95.51% for TC10, 'tl84' and 'horizon', respectively. The average results for both of them are 96.62%.It should be noted that although the LBP^{ri} performs better than LBP^{riu2} at radius 2, the corresponding numbers of the feature sizes are 36, 4118 and 699 252 for (R = 1, P = 8), (R = 2, P = 16) and (R = 3, P = 24), respectively. While the numbers of the feature sizes of the LBP^{riu2} are merely 10, 18 and 26 for (R = 1, P = 8), (R = 2, P = 16) and (R = 3, P = 24), respectively. The variants of the LBP^{riu2}, e.g., the LTP, and the CLBP can achieve much higher classification rates than the LBP^{ri} with a small feature size. Therefore, we can say the LBP^{riu2} is much more efficient for rotation invariant texture classification. The numbers of the feature sizes of the LBC are 9, 17 and 25 for (R = 1, P = 8), (R = 2, P = 16) and (R = 3, P = 24), respectively. Both the LBC and the LBP^{riu2} can achieve impressive performances with the small feature sizes. Thus, we mainly compared our method with the variants of LBP^{riu2}.

C. Experimental Results on CUReT Database

The CUReT database includes 61 classes of textures captured at different viewpoints and illumination orientations. In each class, 92 images were selected from the images shot from a viewing angle of less than 60°. As in [13], [18], N images were randomly chosen as training samples from each class. The remaining (92-N) images were used as test samples. The average classification rates over a hundred random splits are listed in Table II.

We could get the following observation from Table II. The CLBP and the CLBC can get better results than the LTP and the LBP/VAR at every radius. The CLBP performs the best at radius 3 while the CLBC gets the highest classification rate at radius 2. The best results of the CLBP are the classification rates of 95.38%, 91.77%, 85.01% and 76.16% for 46, 23, 12 and 6 training samples, respectively, and the best results of the CLBC are the ones of 95.39%, 91.30%, 85.91% and 75.17% for 46, 23, 12 and 6 training samples, respectively. Similar to the conclusions on the Outex databases, on the average, their performances are at the same level.

It also should be noticed that the separate CLBP_S (CLBP_M) performs much better than the CLBC_S (CLBC_M) on CUReT database. But the performance of the combined CLBP_S_M is similar to the CLBC_S_M. The best results of the CLBP_S_M on CUReT database are the classification rates of 93.94%, 89.88%, 83.95% and 73.23% for 46, 23, 12 and 6 training samples, respectively, and the best results of the CLBC_S_M on CUReT database are the ones of 93.78%, 89.60%, 82.71% and 72.16% for 46, 23, 12 and 6 training samples, respectively. The reason is discussed as follows.

The CLBP_S (LBP^{riu2}) and the CLBC_S (LBC) can be regarded as two ways to describe the local textural distribution. The CLBP_S adopts rotation invariant micro-structure to distinguish different local structures, such as edges, lines, spots, and so on. The CLBC_S merely extracts the local binary grayscale difference information. Although the CLBP_S can improve the classification rate by combining both local binary grayscale difference information and local structural information, in the meantime, the selected rotation invariant structural patterns may be not absolutely invariant to rotation. Both the CLBP_S

TABLE II
CLASSIFICATION RATES (%) ON CUReT DATABASE

	46	23	12	6
LTP (R = 1, P = 8)	85.77	78.49	70.77	60.48
LTP (R = 2, P = 16)	90.21	84.74	76.24	66.75
LTP (R = 3, P = 24)	91.04	85.15	77.88	68.64
LBP/VAR (R = 1, P = 8)	61.55	55.33	49.28	41.96
LBP/VAR (R = 2, P = 16)	55.49	50.76	45.14	39.07
LBP/VAR (R = 3, P = 24)	55.6	51.33	44.5	38.82
CLBP_S (R = 1, P = 8)	80.03	73.07	67.60	58.68
CLBC_S (R = 1, P = 8)	78.82	72.89	66.21	56.88
CLBP_S (R = 2, P = 16)	84.05	79.05	72.01	62.73
CLBC_S (R = 2, P = 16)	79.78	74.42	68.95	60.42
CLBP_S (R = 3, P = 24)	86.06	81.63	75.51	67.00
CLBC_S (R = 3, P = 24)	80.14	74.21	70.57	60.82
CLBP_M (R = 1, P = 8)	74.78	67.86	59.95	57.52
CLBC_M (R = 1, P = 8)	66.61	57.82	58.62	50.12
CLBP_M (R = 2, P = 16)	82.71	75.93	68.32	57.55
CLBC_M (R = 2, P = 16)	73.89	66.05	58.7	50.63
CLBP_M (R = 3, P = 24)	86.59	79.76	72.12	62.81
CLBC_M (R = 3, P = 24)	77.41	68.36	60.53	51.23
CLBP_S_M (R = 1, P = 8)	93.24	88.19	80.43	71.45
CLBC_S_M (R = 1, P = 8)	93.10	86.62	79.88	69.89
CLBP_S_M (R = 2, P = 16)	93.20	89.01	81.93	72.54
CLBC_S_M (R = 2, P = 16)	93.78	89.60	82.71	72.16
CLBP_S_M (R = 3, P = 24)	93.94	89.88	83.95	73.23
CLBC_S_M (R = 3, P = 24)	93.60	89.12	81.57	70.52
CLBP_S/M/C (R = 1, P = 8)	95.19	91.2	83.81	73.44
CLBC_S/M/C (R = 1, P = 8)	94.78	90.12	82.92	72.85
CLBP_S/M/C (R = 2, P = 16)	95.35	91.24	84.66	75.41
CLBC_S/M/C (R = 2, P = 16)	**95.39**	91.30	**85.91**	75.17
CLBP_S/M/C (R = 3, P = 24)	95.38	**91.77**	85.01	**76.16**
CLBC_S/M/C (R = 3,P = 24)	95.26	90.55	84.07	73.18

and the CLBC_S are in very low-dimensions, so that both of them have low local discrimination capability. In CUReT database, images are captured under monotonic illumination and scale transformation, in which condition the rotation invariant "micro-structure" is comparatively robust to rotation. Thus, the CLBP_S performs better than the CLBC_S on the CUReT database since the local structural information improved the performance. When the images are captured under different illumination conditions, i.e., under illumination 'tl84' or 'horizon' in Outex database, the CLBP_S performs similar to or worse than the CLBC_S. That is because the selected rotation invariant structural patterns may be not absolutely robust to rotation under variant illumination conditions, although the local structural information improved the performance at the same time.

The CLBP_M extracts the local grayscale difference information, and it adopts the same encoding process as the CLBP_S. Compared to the CLBC_S, the CLBC_M can extract the 2-order local binary grayscale difference information. Thus, both the CLBP_M and the CLBC_M can indeed extract the grayscale difference discriminative information. The CLBP_M and the CLBC_M both have low discrimination capability in that their feature sizes are quite small. The CLBP_M performs better than the CLBC_M, since the feature sizes of the CLBP_M are slightly higher. By combing the separate descriptors, the CLBP_S_M and the CLBC_S_M can achieve high local discrimination capability to characterize the local textural distribution. Although the separate CLBC_M have lower discriminative power, the CLBC_S_M can describe the local textural distribution almost as well as the CLBP_S_M. In addition, the local micro-structure is not absolutely invariant to rotation. Thus, the joined cases may perform different from the one by separately using the CLBP_S (CLBC_S) or the CLBP_M (CLBC_M).

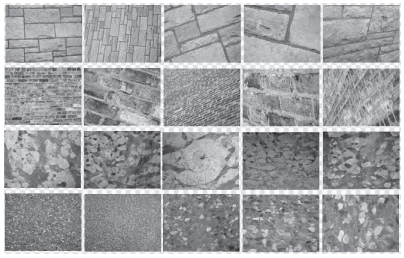

Fig. 5. Textural orientations and scales change a lot in UIUC database. Rows 1–4 show the images of four different classes of the UIUC database.

D. Experimental Results on UIUC Database

The UIUC texture database includes 25 classes and 40 images in each class. The resolution of each image is 640×480 in this database. The database contains materials imaged under significant viewpoint variations. In our texture classification experiments, N training images were randomly chosen from each class while the remaining (40-N) images were used as the test set. The average accuracy over 100 randomly splits are listed in Table III.

We could get the following observation from Table III. Firstly, similar findings to those in CUReT database can be found at radiuses 1, 2, and 3. The CLBP and the CLBC achieve much better results than the LTP and the LBP/VAR. The CLBC performs better than the CLBP at radiuses 2 and 3, while the CLBP get higher classification rates at radius 1. On the average, their performances are still similar to each other. Secondly, although the CLBC gets the best classification rates at radius 2 or 3 on the former datasets, it achieves the best results at radius 4 on UIUC database. Thirdly, the performance of the multi-scale scheme can be improved by expanding the multi-scale levels. When the multi-scale scheme is expanded to radius 5, the multi-scale $\text{CLBP}_{(R=1,2,3,4,5)}$ can reach the classification rates of 91.94%, 90.88%, 87.60% and 80.34% for 20, 15, 10 and 5 training samples, respectively. While the multi-scale $\text{CLBC}_{(R=1,2,3,4,5)}$ can reach the classification rates of 93.68%, 92.04%, 88.86% and 81.67% for 20, 15, 10 and 5 training samples, respectively. Lastly, as illustrated in Fig. 5, it can be found that the textural orientations and scales change a lot in the texture images in UIUC database so that some rotation invariant micro-structures may change after rotation and interpolation. Thus, the separate LBC performs better than the LBP^{riu2} on UIUC database.

E. Discussions

Although the LBC and the CLBC totally abandon the local structural information, their performances on texture databases are almost the same as the LBP's and the CLBP's. This reflects that the mere local binary grayscale information can achieve enough discrimination capability of local texture. The reason why the LBP performs well in rotation invariant texture classification is that the local binary method can effectively characterized the local grayscale distribution, although it is originally designed to characterize the micro-structure.

In this paper, our purpose is to prove that the local grayscale difference information plays a main role in the LBP for rotation invariant texture classification. Some recent related works are mainly involved in how to extract the local rotation invariant structure and ignore the mainly discriminative information in local texture. Compared to the LBC, the LBP variants can improve the classification rate by using local micro-structural information sometimes. But in the meantime, the selected micro-structure may be not absolutely rotation

TABLE III
CLASSIFICATION RATES (%) ON UIUC DATABASE

	20	15	10	5
LTP (R = 1, P = 8)	67.16	64.29	58.20	48.15
LTP (R = 2, P = 16)	79.25	75.80	70.77	60.34
LTP (R = 3, P = 24)	82.34	79.10	73.94	62.19
LBP/VAR(R = 1, P = 8)	66.61	63.98	58.49	50.37
LBP/VAR (R = 2, P = 16)	73.31	70.58	66.04	57.03
LBP/VAR (R = 3, P = 24)	75.01	71.94	66.86	57.55
CLBP_S (R = 1, P = 8)	54.78	51.85	46.79	40.53
CLBC_S (R = 1, P = 8)	55.61	51.11	46.69	39.85
CLBP_S (R = 2, P = 16)	61.04	55.84	51.77	41.88
CLBC_S (R = 2, P = 16)	62.39	59.17	53.07	43.37
CLBP_S (R = 3, P = 24)	64.11	60.11	54.67	44.45
CLBC_S (R = 3, P = 24)	66.90	63.48	57.46	47.19
CLBP_M (R = 1, P = 8)	57.52	54.14	50.11	40.95
CLBC_M (R = 1, P = 8)	52.12	49.84	45.51	39.04
CLBP_M (R = 2, P = 16)	72.12	68.99	64.47	57.06
CLBC_M (R = 2, P = 16)	67.1	64.42	59.01	50.67
CLBP_M (R = 3, P = 24)	74.45	71.47	65.21	56.72
CLBC_M (R = 3, P = 24)	69.33	66.63	60.62	51.68
CLBP_S_M (R = 1, P = 8)	81.80	78.55	74.8	64.84
CLBC_S_M (R = 1, P = 8)	82.40	78.86	74.88	65.28
CLBP_S_M (R = 2, P = 16)	87.87	85.07	80.59	71.64
CLBC_S_M (R = 2, P = 16)	88.51	86.31	82.04	73.16
CLBP_S_M (R = 3, P = 24)	89.18	87.42	81.95	72.53
CLBC_S_M (R = 3, P = 24)	89.72	87.68	83.92	75.16
CLBP_S/M/C (R = 1, P = 8)	87.64	85.70	82.65	75.05
CLBC_S/M/C (R = 1, P = 8)	87.83	85.66	82.35	74.57
CLBP_S/M/C (R = 2, P = 16)	91.04	89.42	86.29	78.57
CLBC_S/M/C (R = 2, P = 16)	91.04	89.66	86.63	79.48
CLBP_S/M/C (R = 3, P = 24)	91.19	89.21	85.95	78.05
CLBC_S/M/C (R = 3, P = 24)	91.39	90.10	86.45	79.75
CLBP_S/M/C (R = 4, P = 32)	90.20	88.96	85.36	76.47
CLBC_S/M/C (R = 4, P = 32)	91.79	89.77	86.67	79.78
CLBP_S/M/C (R = 5, P = 40)	90.16	88.8	85.04	76.24
CLBC_S/M/C (R = 5, P = 40)	91.35	89.84	86.13	78.13
CLBP_S/M/C (R = 6, P = 48)	89.80	87.52	84.40	76.15
CLBC_S/M/C (R = 6, P = 48)	90.88	89.42	86.18	78.36
Multiscale CLBP (R = 1, 2, 3)	91.57	89.84	86.73	78.42
Multiscale CLBC (R = 1, 2, 3)	92.42	90.66	87.75	80.22
Multiscale CLBP (R = 1, 2, 3, 4, 5)	91.94	90.88	87.60	80.34
Multiscale CLBC (R = 1, 2, 3, 4, 5)	**93.68**	**92.04**	**88.86**	**81.67**

invariant, especially when the images are captured under significant illumination and viewpoint variations.

Generally, the number of the specified rotation invariant local patterns is too few to contain abundant structural information since rotation invariance is necessary in texture classification. When rotation invariance is not required for some practical applications, e.g., for face recognition problem, the LBP^{u2} is still a very effective local operator containing both local structural information and local binary grayscale difference information.

V. CONCLUSION

In this paper, we proposed a novel local operator of Local Binary Count (LBC), where the LBC abandons the structural information. Although the LBC codes don't represent visual micro-structure, the LBC is proved to be efficient for rotation invariant texture classification. The micro-structure can improve the classification rate sometimes, but the micro-structure is not absolutely invariant to rotation, especially when the illumination conditions or the textural scales change a lot. Then a completed LBC (CLBC) was also proposed to enhance the binary grayscale difference information extracted in local textures.

ACKNOWLEDGMENT

The authors would like to sincerely thank the Center for Machine Vision Research and Z. Guo for sharing the source codes of the local binary pattern and compound local binary pattern.

REFERENCES

[1] L. S. Davis, "Polarograms - a new tool for image texture analysis," *Pattern Recognit.*, vol. 13, no. 3, pp. 219–223, 1981.
[2] J. Duvernoy, "Optical digital processing of directional terrain textures invariant under translation, rotation, and change of scale," *Appl. Opt.*, vol. 23, no. 6, pp. 828–837, 1984.
[3] R. K. Goyal, W. L. Goh, D. P. Mital, and K. L. Chan, "Scale and rotation invariant texture analysis based on structural property," in *Proc. IEEE Int. Conf. Ind. Electron., Control, Instrum.*, vols. 1–2. Nov. 1995, pp. 1290–1294.
[4] G. Eichmann and T. Kasparis, "Topologically invariant texture descriptors," *Comput. Vis. Graph. Image Process.*, vol. 41, no. 3, pp. 267–281, Mar. 1988.
[5] R. L. Kashyap and A. Khotanzad, "A model-based method for rotation invariant texture classification," *IEEE Trans. Pattern Anal. Mach. Intell.*, vol. 8, no. 4, pp. 472–481, Jul. 1986.
[6] F. S. Cohen, Z. G. Fan, and M. A. Patel, "Classification of rotated and scaled textured images using Gaussian Markov random field models," *IEEE Trans. Pattern Anal. Mach. Intell.*, vol. 13, no. 2, pp. 192–202, Feb. 1991.
[7] J. L. Chen and A. Kundu, "Rotation and gray scale transform invariant texture recognition using hidden Markov model," in *Proc. Int. Conf. Acoust., Speech, Signal Process.*, vols. 1–5. 1992, pp. C69–C72.
[8] R. Porter and N. Canagarajah, "Robust rotation invariant texture classification," in *Proc. IEEE Int. Conf. Acoust., Speech, Signal Process.*, vols. 1–5. Jun. 1997, pp. 3157–3160.
[9] T. Ojala, M. Pietikainen, and T. Maenpaa, "Multiresolution gray-scale and rotation invariant texture classification with local binary patterns," *IEEE Trans. Pattern Anal. Mach. Intell.*, vol. 24, no. 7, pp. 971–987, Jul. 2002.
[10] M. Heikkilä, M. Pietikäinen, and C. Schmid, "Description of interest regions with center-symmetric local binary patterns," in *Proc. Comput. Vis., Graph. Image Process.*, vol. 4338. 2006, pp. 58–69, DOI: 10.1007/11949619_6.
[11] S. Liao, M. W. K. Law, and A. C. S. Chung, "Dominant local binary patterns for texture classification," *IEEE Trans. Image Process.*, vol. 18, no. 5, pp. 1107–1118, May 2009.
[12] X. Y. Tan and B. Triggs, "Enhanced local texture feature sets for face recognition under difficult lighting conditions," *IEEE Trans. Image Process.*, vol. 19, no. 6, pp. 1635–1650, Jun. 2010.
[13] Z. H. Guo, L. Zhang, and D. Zhang, "A completed modeling of local binary pattern operator for texture classification," *IEEE Trans. Image Process.*, vol. 19, no. 6, pp. 1657–1663, Jun. 2010.
[14] F. Khellah, "Texture classification using dominant neighborhood structure," *IEEE Trans. Image Process.*, vol. 20, no. 11, pp. 3270–3279, Nov. 2011.
[15] T. Ojala, T. Maenpaa, M. Pietikainen, J. Viertola, J. Kyllönen, and S. Huovinen, "Outex - new framework for empirical evaluation of texture analysis algorithms," in *Proc. 16th Int. Conf. Pattern Recognit.*, vol. 1. 2002, pp. 701–706.
[16] K. J. Dana, B. Van Ginneken, S. K. Nayar, and J. J. Koenderink, "Reflectance and texture of real-world surfaces," *ACM Trans. Graph.*, vol. 18, no. 1, pp. 1–34, Jan. 1999.
[17] M. Varma and A. Zisserman, "A statistical approach to material classification using image patch exemplars," *IEEE Trans. Pattern Anal. Mach. Intell.*, vol. 31, no. 11, pp. 2032–2047, Nov. 2009.
[18] S. Lazebnik, C. Schmid, and J. Ponce, "A sparse texture representation using local affine regions," *IEEE Trans. Pattern Anal. Mach. Intell.*, vol. 27, no. 8, pp. 1265–1278, Aug. 2005.
[19] T. Ahonen and M. Pietikäinen, "Image description using joint distribution of filter bank responses," *Pattern Recognit. Lett.*, vol. 30, no. 4, pp. 368–376, 2009.
[20] H. Lategahn, S. Gross, T. Stehle, and T. Aach, "Texture classification by modeling joint distributions of local patterns with Gaussian mixtures," *IEEE Trans. Image Process.*, vol. 19, no. 6, pp. 1548–1557, Jun. 2010.